ECS Transactions, 61 (11) 13-23 (2014)
10.1149/06111.0013ecst ©The Electrochemical Society

# Analytical modeling of PEM fuel cell gas diffusion layers deformation under compression: Part2-Nonlinear behaviour region

V. Norouzifard [a], M. Bahrami [a]

[a] Laboratory for Alternative Energy Conversion (LAEC), Mechatronic Systems Engineering, Simon Fraser University, BC, Canada, V3T 0A3

In the Proton exchange membrane PEM fuel cell stack, the porous gas diffusion layer (GDL) provides mechanical support for the membrane assembly against the compressive loads imposed by bipolar plates. In this paper, using assumption of existing gap between the fibers in the GDL micro-structure, an analytical model proposed in first part of this study for linear region is extended to predict the GDL nonlinear mechanical behaviour in low compressive pressures. The present unit cell model covers salient microstructural parameters and properties of the fibrous porous medium including: carbon fiber diameter, elastic modulus, pore size distribution, gap size distribution between fibers. A comparison between the present model and the GDL stress-strain data shows that the assumption of closing gap between the fibers during compression can accurately describe the GDL nonlinear behaviour. The proposed model also provides useful information about the microstructural properties of the GDL during compression such as gap distribution between fibers that can be used in the GDL transport properties prediction.

## Introduction

One of the main components of the membrane electrode assembly (MEA) is a highly fibrous porous media called the gas diffusion layer (GDL), which is made from carbon fibers in the form of paper or cloth. Beside of the GDL's transportation duties in a fuel cell stack such as: providing electronic conductivity between components, reactant access to catalyst layers as well as removing generated heat and reaction products, it acts as a mechanical support for the MEA components against the compressive loads applied by bipolar plates (1). An appropriate contact between the membrane layers is essential with low thermal and electrical contact resistances to ensure that the heat and electricity generated during the cell operation will be collected properly. During cell assembling and operation, compressive loads act on the MEA layers. The MEA is compressed between bipolar plates during assembling process to ensure proper contact between layers and also to seal the cell. Extra compressive load also acts on the GDL due to the hygro-thermal loading and the membrane swelling (2–8) during cell operation. The flexible, porous microstructure of the GDL deforms considerably when subjected to such compressive loads. The GDL properties such as porosity, permeability, diffusivity, electrical and thermal bulk conductivities and contact resistances change significantly during the GDL compression (9). Changing in the GDL properties can significantly affect the transport phenomena, overall performance and life of the fuel cell stack. Therefore, the mechanical

behaviour of the GDL under compression should be well understood. In recent years, a number of studies have focused on the experimental and analytical investigation of the mechanical (10–15) as well as thermal (1,16–19) and electrical (11) behaviour of GDL and its interfacial interaction (1,9,17,20–23) under compressive loading.

The majority of the existing studies on the GDL's mechanical deformation were focused on numerical simulation of the inhomogeneous compression of the GDL under the bipolar plates' ribs using finite element method (FEM) (1, 5, 7, 24–26). In all of these studies, commercial FEM software was utilized for mechanical modeling. The GDL mechanical behaviour modeling is the most important part of such numerical simulations. As mentioned in the first part of this study, the mechanical behaviour of GDL can be divided into two regions; linear and nonlinear region. For compressive loads smaller than a critical value, the GDL mechanical deformation is nonlinear and compression modulus increases by increasing the load. Beyond the critical pressure, the modulus remains constant and the GDL mechanical behaviour changes to linear.

Nitta (27) determined compressive stress of 1 MPa to be the critical stress for SGL 10 BA GDL and related the linear deformation region between pressures 1 to 3.5 MPa to the crushing of the hydrophobic pores in the GDL. Although compression pressure applied by bipolar plates on the MEA usually is higher than 1 MPa, the GDL material behaviour is also needed to be determined in compressive loads under 1 MPa for the GDL deformation simulation under the bipolar plates' ribs because of non-uniform stress distribution in the GDL. Garcia-Salaberri et. al. (9) divided the GDL's through plane compressive mechanical response into the three regions; small strain hardening, constant modulus, and large strain hardening. The first and second regions are as same as the non-linear and linear deformation regions which are explained above. The third one, large strain hardening, occurs in stress and strain higher than 3.5 MPa which is higher than the loads usually applied on the MEA during fuel cell normal operation. Thus, large strain hardening is not focus of the present study.

Figure 1a shows the microstructure of a GDL from side view captured by scanning electron microscope (SEM). This image shows initial gaps between carbon fibers in the GDL structure. The initial gaps are responsible for the variable compression modulus of the GDL in compressive loads less than 1 MPa. GDL compression in the linear region has been investigated in the first part of this study. It is assumed that the bending of carbon fibers is the main mechanism of the GDL deformation under compression. In nonlinear region, i.e., compressive pressures less than 1 MPa, the fiber bending is still the main deformation mechanism of the GDL. In addition, in this region, closing the initial gaps between carbon fibers changes the average length of the unit cells during compression. The average length of the bending unit is called the effective unit cell length in this paper. As the GDL is compressed, the initial gaps are closed and number of contact points between the fibers increase. Thus the effective unit cell length decreases. Figure 1b also shows the explained mechanism for the unit cell length change in the nonlinear region. The effective unit cell length reaches a minimum value in the pressure around 1 MPa and remains constant beyond this pressure.

Garcia-Salaberri *et. al.* (9) created an empirical nonlinear stress-strain relationship by curve fitting the widespread data sets available in the literature. Although such empirical relationships can resolve the FEM models requirements for definition of the GDL material behaviour, they do not explain the dependency of the materials mechanical behaviour on the microstructure specifications. The aim of this study is to develop an analytical model to determine the GDL mechanical behaviour in the linear and nonlinear regions based on the microstructural properties of the GDL material. The linear

behaviour of the GDL was modeled in the first part of this study based on the unit cell approach and carbon fibers bending.

In this paper the linear model developed in the first part is extended to the nonlinear region. The mechanistic analytical model predicts the compressive stress-strain relationship of carbon paper GDLs using only their microstructural parameters such as fiber diameter and fibre elastic modulus, pore size distribution and porosity. Random and complex microstructure of the GDL is modelled by unit cell approach which has been successfully used by our group for modeling GDL's thermal conductivity, thermal contact resistance, and permeability (1,18,28,29). Carbon fiber bending is considered as the main deformation mechanism at the unit cell level and overall GDL deformation is calculated from the summation of all unit cells' deformations. The compressive modulus variation in the nonlinear region of the GDL deformation is modeled based on the initial gap distribution between the carbon fibers. Therefore, a correlation for the unit cell length versus the compressive pressure is developed based on the initial gap distribution. The initial gap distribution statistical parameters are estimated by fitting experimental stress-strain data on the proposed model.

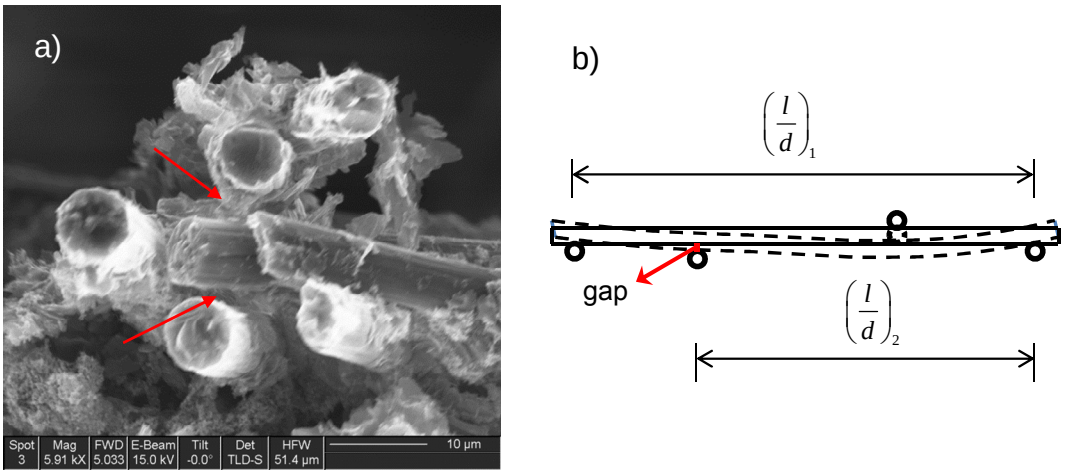


Figure 1. a) SEM image of the fibrous microstructure of a PEMFC gas diffusion layer side view; GDL: SGL 24AA immersed in the epoxy resin and cut by Microtome, gaps between fibers are marked, and b) Effective unit cell length changes in low pressures due to the existing gaps between fibers (dashed lines show fiber location after compression).

## Analytical model development

In the first part of this study, the mechanical behaviour of the paper based GDL materials are modeled successfully for the linear region in which the GDL is compressed by pressures higher than 1 MPa. In the linear region, it is assumed that all carbon fibers in the GDL structure are in contact with their top and bottom neighbour fibers. In the case that all fibers are in contact (no gap in the contact points), the effective unit cell length can be estimated by optical measurements using top view microscopic images of GDL as reported in the first part. After analysis of the GDL layered structure deformation, the following equation has been developed to calculate the non-dimensionalized effective unit cell length:

$$\left(\frac{l}{d}\right)_{eff} = \left(\frac{\mu_l^3 \mu_{A_{pore}}}{\varepsilon \mu_d^5 \left(1+6C_l^2\right)\left(1+6C_d^2\right)}\right)^{\frac{1}{5}} \quad [1]$$

where, $\mu$ and $C$ are the mean and coefficient of variation, $l$, $d$, $A_{pore}$ and $\varepsilon$ are unit cell length, fiber diameter, pore area, and GDL porosity, respectively. Also, a new compact relationship between the compressive strain, $e$, and stress, $\sigma$, has been presented in the first part of this study for GDL linear compression region as follows:

$$e = \frac{16\sigma}{105\pi E}\left(\frac{l}{d}\right)_{eff}^5 \quad [2]$$

where, $E$ is the carbon fibers elastic modulus that can be found in literature (30).

To develop an analytical model for the nonlinear region of the GDL compression, the gaps between fibers should be considered in the model. Figure 1b schematically shows the proposed bending mechanism in low pressure range in a unit cell due gap reduction. The solid and dashed lines in Figure 1b show the fiber deflections before and after compression in the low range pressure, respectively. As such, the bent fiber deformation fills the gaps between the fibers, thus the effective unit cell length ($l$) is changed. A relationship between the effective unit cell length and number of unit cells is needed to explain the GDL nonlinear mechanical behaviour as a function of compressive strain. The procedure of development of the nonlinear GDL deformation model is explained below.

According to the first part of this study, the following equation has been derived to calculate number of unit cells in one layer of GDL:

$$N = \frac{A_s \varepsilon}{\mu_{A_{pore}}} \quad [3]$$

where, $A_s$ , $\varepsilon$ and $\mu_{A_{pore}}$ are the sample area, porosity, and pore area mean value, respectively. Figure 2 schematically shows a pore in the GDL unit cell model. The pore area can be calculated readily by:

$$\mu_{A_{pore}} = \mu_{l_1} . \mu_{l_2} . \mu_{\sin\theta} \quad [4]$$

where, $l_1$ and $l_2$ are randomly distributed unit cell lengths and $\theta$ is the angle between carbon fibers, respectively. Sets of $l_1$ and $l_2$ values are subsets of $l$ values. Thus, the following relationship can be written between mean values of $l_1$ , $l_2$ and $l$:

$$\mu_l = \frac{\mu_{l_1} + \mu_{l_2}}{2} \quad [5]$$

$l_1$ and $l_2$ are also related through aspect ratio as following:

$$\mu_{l_1} = \mu_{AP}.\mu_{l_2} \quad [6]$$

where, *AP* is the aspect ratio and can be defined as:

$$AP = \frac{l_1}{l_2} \quad [7]$$

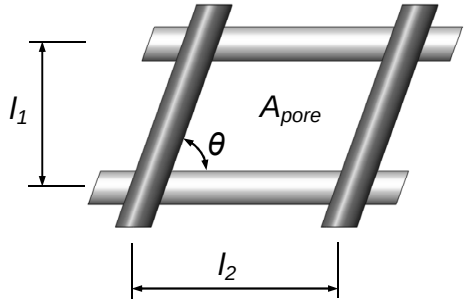


Figure 2. Schematic of a pore in the present unit cell model of GDL.

According to the optical measurements performed in our group in previous studies (18) on the GDL properties characterization, $\theta$ and *AP* are randomly distributed variables. Substituting Eqs. [5] and [6] in Eq. [4] leads to:

$$\mu_{A_{pore}} = \frac{4\mu_{AP}\mu_{\sin\theta}}{\left(1+\mu_{AP}\right)^2}\mu_l^2 \quad [8]$$

If the mean value of the aspect ratio is assumed to be constant during the GDL compression, comparing Eq. [8] with Eq. [3] yields:

$$N \propto \frac{1}{\mu_l^2} \quad [9]$$

The coefficient of variation for unit cell length is also assumed to be constant during compression. Then, substituting Eq. [8] in Eq. [1] and assuming constant coefficient of variation for the unit cell length during deformation result:

$$\left(\frac{l}{d}\right)_{eff} \propto \mu_l \quad [10]$$

From Eqs. [9] and [10], one can find a relationship between the non-dimensional effective unit cell length and the number of unit cells:

$$\left(\frac{l}{d}\right)_{eff} \propto \sqrt{\frac{1}{N}} \quad [11]$$

There are number of unit cells in an uncompressed GDL, $N_{initial}$, which increase during compression of the GDL because of the closing-gaps mechanism between fibers/layers. Thus, the number of unit cells as a function of strain, $N(e)$, can be expressed as:

$$N(e) = N_{initial} + N_{closed\ gaps} \quad [12]$$

Dividing Eq. [12] to the total number of unit cells, $N_{total}$, (number of unit cells in the linear region) and considering the fact that $N_{total}$ is equal to the summation of $N_{initial}$ and total number of gaps, $N_{total\ gaps}$, one will find:

$$\frac{N(e)}{N_{total}} = \frac{N_{initial}}{N_{total}} + \left(1 - \frac{N_{initial}}{N_{total}}\right)\frac{N_{closed\ gaps}}{N_{total\ gaps}} \quad [13]$$

Although, there are number of probability distributions such as Gaussian, Gamma, Beta, and Weibull, which can be assumed for distribution of the gap lengths between carbon fibers, Gaussian distribution is used in the present study, as it do not add more than two unknown parameter to the present equations. The other distributions mentioned above add equal or more than three unknown parameters to the equations that it cause the equations is more to be indeterminate and cannot be solved by the present method. During the GDL compression, the gaps which are shorter than the GDL layer's deformation are closed. The ratio of closed gaps to total gaps as a function of GDL per layer deformation, $\delta_l$, can be written as:

$$\frac{N_{closed\ gaps}}{N_{total\ gaps}} = \frac{1}{2} + \frac{1}{2} erf\left(\frac{\delta_l - \mu_g}{S_g\sqrt{2}}\right) \quad [14]$$

where, $\mu_g$ and $S_g$ are the mean and standard deviation of the gap random (Gaussian) distribution, respectively. Deformation per layer is the product of strain multiplied by layer thickness (assumed to be equal with the carbon fiber diameter), then:

$$\delta_l = ed \quad [15]$$

where, $e$ and $d$ are strain and carbon fiber diameter. Substituting Eqs. [14] and [15] in Eq. [13] gives:

$$\frac{N(e)}{N_{total}} = \frac{N_{initial}}{N_{total}} + \left(1 - \frac{N_{initial}}{N_{total}}\right)\left(\frac{1}{2} + \frac{1}{2} erf\left(\frac{ed - \mu_g}{S_g\sqrt{2}}\right)\right) \quad [16]$$

Experimental stress-strain data from the first part of this study and the literature (27) for some of off-the-shelf GDLs are substituted in Eq. [2]. Then, the non-dimensional effective unit cell length is calculated versus the compressive stress. Figure 3 shows the ratio of the effective unit cell length to linear effective unit cell length versus the pressure. From Figure 3, the ratio of $(l/d)_{initial}/(l/d)_{linear}$ for SEGRACET and TORAY uncompressed GDLs are about 1.4 and 1.7, respectively. From Eq. [11], corresponding

$N_{initial}/N_{total}$ are 0.50 and 0.34 for SEGRACET and TORAY GDLs. The effective compression modulus of the GDL can be defined as:

$$E^* = \frac{d\sigma}{de} \quad [17]$$

where, $d(\cdot)$ is the differential operator. Combining Eqs. [17], [16], [11] and [2], one can find the following for the compression modulus:

$$E^*(e) = \frac{105\pi E}{16\left(\frac{l}{d}\right)_{linear}^5}\left(A + Berf\left(\frac{ed-\mu_g}{S_g\sqrt{2}}\right)\right)^{\frac{5}{2}} \quad [18]$$

where, $A$ and $B$ are constants. Using calculated values for $N_{initial}/N_{total}$ from experimental data yields $A$= 0.75 and $B$= 0.25 for SEGRACET and 0.67 and 0.33 for TORAY GDLs, respectively. $(l/d)_{linear}$ was calculated by statistical processing of optically measured data in the first part of this study. Table I lists $(l/d)_{linear}$ for the GDLs considered in this paper.

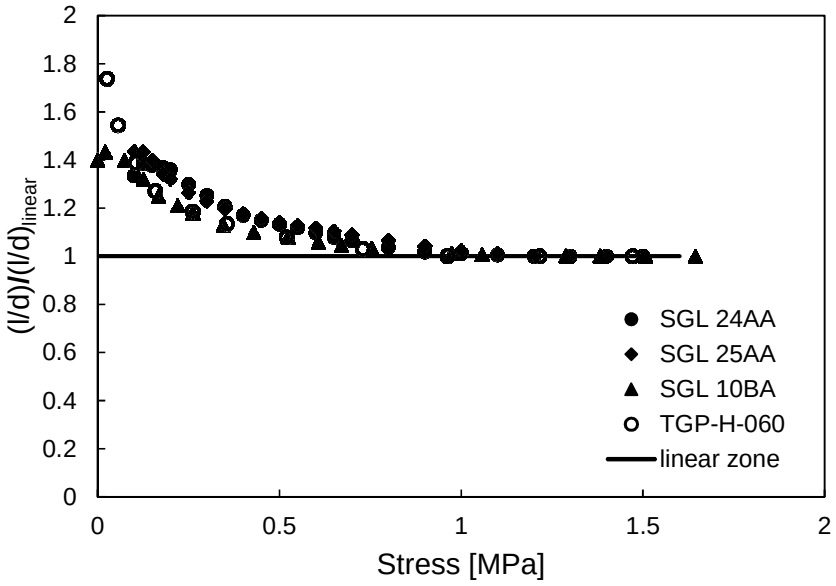


Figure 3. The ratio of the non-dimensional effective unit cell length to linear non-dimensional effective unit cell length versus the pressure, Data are collected from the first part of this study for SGL 24AA and 25AA, (11) for TGP-H-60 and (27) for SGL 10BA, respectively.

**TABLE I.** The mechanical properties and geometrical characteristics of the SIGRACET and TORAY GDL samples used in this study.

| GDL type | $\varepsilon$ (%) | $\mu_l$ (μm) | $C_l$ | $\mu_d$ (μm) | $C_d$ | $E$ (GPa) | $\left(l/d\right)_{linear}$ |
|---|---|---|---|---|---|---|---|
| SGL 24AA | 88 (18) | 130 | 0.414 | 6.95 | 0.0812 | 225 (30) | 13.12 |
| SGL 25AA | 92 (18) | 135.8 | 0.433 | 6.95 | 0.0812 | 225 (30) | 13.98 |
| SGL 10BA | 88 (27) | 118.5 | 0.376 | 6.95 | 0.0812 | 225 (30) | 14.18 |
| TGP-H-060 | 78 (18) | 97.24 | 0.387 | 6.13 | 0.106 | 225 (30) | 12.98 |

## Results and discussion

In the previous section, a nonlinear relationship, Eq. [18], was developed to predict GDL's compressive modulus as a function of strain and the gap distribution statistical characteristics. To predict the compressive modulus, Eq. [18] needs the statistical parameters of gap distribution. Direct measurement of the gap distribution between carbon fiber in the GDL structure is not an easy task. In the present study, the gap distribution parameters are estimated by fitting the available experimental data on the model. This method presents valuable information about gap distribution in the GDL media from the stress-strain data, which can be measured relatively easily.

According to Figure 3, the linear region of the GDL deformation starts in 1 MPa compressive pressure, as proposed by Nitta (27). Thus, it can be assumed that almost all existing gaps between carbon fibers are closed at this pressure. Compression per layer in this pressure is equal to $e_1 d$ where, $e_1$ is the GDL strain in 1 MPa compressive pressure. Therefore, it can be assumed that the gaps length are distributed between zero and $e_1 d$. To fit a Gaussian distribution for gaps in the mentioned range, i.e. zero to $e_1 d$, two parameters are defined as:

$$\alpha = \frac{\mu_g}{e_1 d} \qquad [19]$$

$$\beta = \frac{\mu_g}{S_g} \qquad [20]$$

To find a suitable gap distribution, it is necessary to determine these parameters, $\alpha$ and $\beta$, as the difference between the experimental compression modulus and the predicted results are minimized. The normalized root mean square of difference can be calculated as:

$$NRMS_{E^*} = \frac{\sqrt{\frac{\sum\left(E^*_{Exp.} - E^*_{Model}\right)^2}{n}}}{\left(E^*_{Exp.}\right)_{\max} - \left(E^*_{Exp.}\right)_{\min}} \qquad [21]$$

Optimum values of $\alpha$ and $\beta$ corresponding to the considered GDLs are listed in Table II. Figure 4 compares the predicted compressive modulus of the studied GDL

samples based on the optimum $\alpha$ and $\beta$ versus experimental data. The solid line in Figure 4 shows the ideal case in which the model results are exactly matched with the data. As seen in Figure 4, the relative difference between the data and the model is reasonably low, maximum relative difference 7.54%. It means that the proposed mechanism for GDL deformation can explain the GDL compressive modulus variation in low pressures with reasonable accuracy.

**TABLE II.** Calculated gap distribution characteristics of the SIGRACET and TORAY GDL samples used in this study.

| | Optimum $\alpha$ and $\beta$ | | For optimum $\alpha$ and $\beta$ | | | For average $\alpha$ and $\beta$ $\alpha = 0.61, \beta = 2.3$ | | |
|---|---|---|---|---|---|---|---|---|
| GDL type | $\alpha$ | $\beta$ | $S_g$ (μm) | $\mu_g$ (μm) | $NRMS_{E^*}$ (%) | $S_g$ (μm) | $\mu_g$ (μm) | $NRMS_{E^*}$ (%) |
| SGL 24AA | 2.36 | 0.66 | 0.278 | 0.868 | 5.71 | 0.286 | 0.802 | 7.96 |
| SGL 25AA | 2.28 | 0.63 | 0.412 | 1.18 | 7.54 | 0.408 | 1.14 | 7.93 |
| SGL 10BA | 2.1 | 0.53 | 0.416 | 0.928 | 3.58 | 0.380 | 1.06 | 8.12 |
| TGP-H-060 | 2.44 | 0.6 | 0.284 | 0.831 | 4.10 | 0.301 | 0.84 | 4.74 |

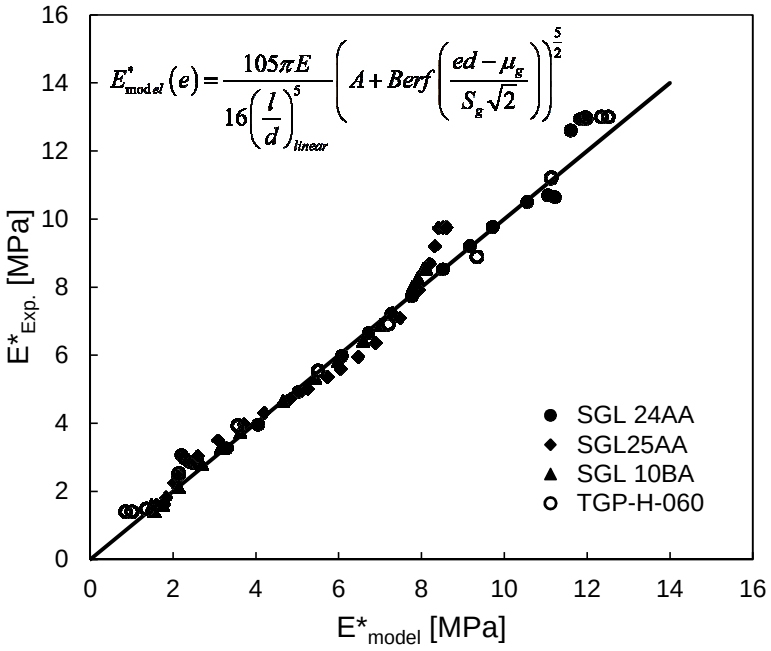


Figure 4. Compressive modulus of the studied GDL samples based on the optimum $\alpha$ and $\beta$ versus the experimental modulus, Data are collected from the first part of this study for SGL 24AA and 25AA, (11) for TGP-H-60 and (27) for SGL 10BA, respectively.

As shown in Table II, the calculated $\alpha$ and $\beta$ for the GDL types are close, therefore, the average value of the parameters can be proposed to calculate gap distribution characteristics from stress-strain data. The normalized root mean squares of the differences are also listed in Table II. Although, $NRMS_{E^*}$ listed in Table II increases when the average value of the calculated $\alpha$ and $\beta$ is used, the maximum value of

$NRMS_{E^*}$ increases from 7.54% to 8.12% and still is reasonably low. Thus, it can be conclude that the model also presents a good prediction of the GDL mechanical behaviour with the average $\alpha$ and $\beta$. Figure 5 shows the reconstructed stress-strain graphs by the proposed model comparing with the original data.

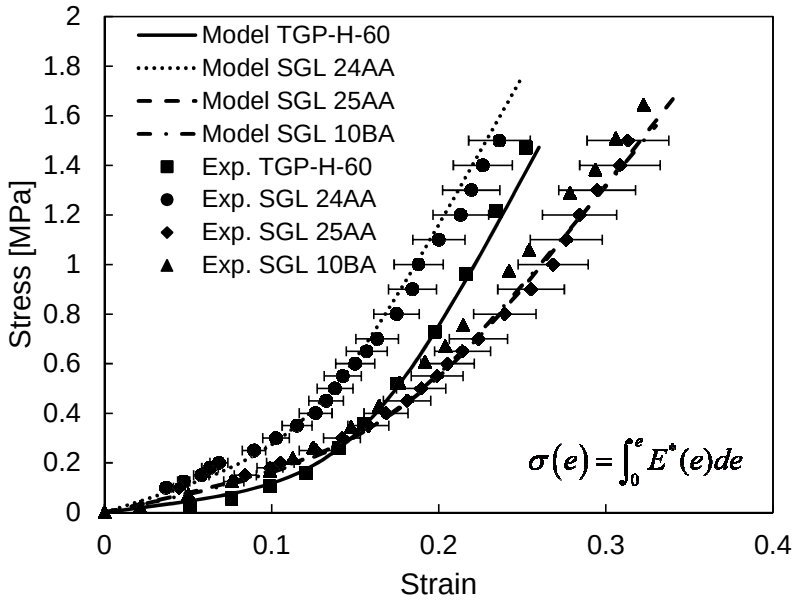


Figure 5. Experimental stress-strain data and reconstructed stress-strain graphs by model, Data are collected from the first part of this study for SGL 24AA and 25AA, (11) for TGP-H-60 and (27) for SGL 10BA, respectively.

## Conclusion

In this paper, a novel analytical model was developed to predict the nonlinear mechanical behaviour of carbon fiber based GDLs under compressive loading. A unit cell approach was used to model the geometry of the GDL fibrous porous microstructure. Bending of carbon fibers and closing the initial gaps between carbon fibers/layers were considered as the mechanisms responsible for the nonlinear GDL compression behaviour. The present model takes into account salient GDL microstructural characteristics and properties such as carbon fibers diameter, elastic modulus, pore size distribution, and porosity. The statistical characteristics of the Gaussian distribution proposed for the gap length distribution were calculated by fitting the available experimental stress-strain data on the developed model. Comparing the calculated compressive modulus of the GDL using the model and the experimental data, we showed that the proposed mechanism for GDL deformation could explain the GDL compressive modulus variation in low pressures with good accuracy. The present model also proposes a methodology that can be used in the future studies of the GDL properties characterization to calculate the GDL microstructure parameters such as gap distribution from the stress-strain data.

## References

1. E. Sadeghi, N. Djilali, and M. Bahrami, *J. Power Sources*, **195**, 8104–8109 (2010).
2. A. Kusoglu, M. H. Santare, A. M. Karlsson, S. Cleghorn, and W. B. Johnson, *J. Electrochem. Soc.*, **157**, B705 (2010).

3. A. Kusoglu, A. M. Karlsson, M. H. Santare, S. Cleghorn, and W. B. Johnson, *J. Power Sources*, **161**, 987–996 (2006).
4. R. Solasi, Y. Zou, X. Huang, K. Reifsnider, and D. Condit, *J. Power Sources*, **167**, 366–377 (2007).
5. Z. Lu, C. Kim, A. M. Karlsson, J. C. Cross, and M. H. Santare, *J. Power Sources*, **196**, 4646–4654 (2011).
6. M. N. Silberstein and M. C. Boyce, *J. Power Sources*, **196**, 3452–3460 (2011).
7. Y. Zhou, G. Lin, a. J. Shih, and S. J. Hu, *J. Power Sources*, **192**, 544–551 (2009).
8. A. Kusoglu, A. M. Karlsson, M. H. Santare, S. Cleghorn, and W. B. Johnson, *J. Power Sources*, **170**, 345–358 (2007).
9. P. A. García-Salaberri, M. Vera, and R. Zaera, *Int. J. Hydrogen Energy*, **36**, 11856–11870 (2011).
10. S. Escribano, J.-F. Blachot, J. Ethève, A. Morin, and R. Mosdale, *J. Power Sources*, **156**, 8–13 (2006).
11. J. Kleemann, F. Finsterwalder, and W. Tillmetz, *J. Power Sources*, **190**, 92–102 (2009).
12. K. K. Poornesh, C. D. Cho, G. B. Lee, and Y. S. Tak, *J. Power Sources*, **195**, 2718–2730 (2010).
13. V. Radhakrishnan and P. Haridoss, *Mater. Des.*, **32**, 861–868 (2011).
14. M. F. Serincan and U. Pasaogullari, *J. Power Sources*, **196**, 1314–1320 (2011).
15. I. Nitta, T. Hottinen, O. Himanen, and M. Mikkola, *J. Power Sources*, **171**, 26–36 (2007).
16. E. Sadeghi, M. Bahrami, and N. Djilali, *J. Power Sources*, **179**, 200–208 (2008).
17. E. Sadeghi, N. Djilali, and M. Bahrami, *J. Power Sources*, **196**, 246–254 (2011).
18. H. Sadeghifar, M. Bahrami, and N. Djilali, *J. Power Sources*, **233**, 369–379 (2013).
19. I. Nitta, O. Himanen, and M. Mikkola, *Fuel Cells*, **8**, 111–119 (2008).
20. Z. Wu, S. Wang, L. Zhang, and S. J. Hu, *J. Power Sources*, **189**, 1066–1073 (2009).
21. Z. Wu, Y. Zhou, G. Lin, S. Wang, and S. J. Hu, *J. Power Sources*, **182**, 265–269 (2008).
22. Y. Zhou, G. Lin, a. J. Shih, and S. J. Hu, *J. Power Sources*, **163**, 777–783 (2007).
23. I. Nitta, O. Himanen, and M. Mikkola, *Electrochem. commun.*, **10**, 47–51 (2008).
24. P. Zhou, C. W. Wu, and G. J. Ma, *J. Power Sources*, **159**, 1115–1122 (2006).
25. P. Zhou, C. W. Wu, and G. J. Ma, *J. Power Sources*, **163**, 874–881 (2007).
26. P. Zhou and C. W. Wu, *J. Power Sources*, **170**, 93–100 (2007).
27. I. Nitta, thesis, Helsinki University of Technology (2008).
28. A. Tamayol, F. McGregor, and M. Bahrami, *J. Power Sources*, **204**, 94–99 (2012).
29. A. Tamayol, K. W. Wong, and M. Bahrami, *Phys. Rev. E*, **85**, 026318 (2012).
30. M. Mathias, J. Roth, J. Fleming, and W. Lehnert, in *Handbook of fuel cell*,, vol. 3, John Wiley & Sons (2003).